HHS Public Access

Author manuscript

Immunohorizons. Author manuscript; available in PMC 2020 June 25.

Published in final edited form as:

Immunohorizons. ; 3(1): 1–12. doi:10.4049/immunohorizons.1800056.

Identification of novel respiratory syncytial virus CD4+ and CD8+ T cell epitopes in C57BL/6 mice

Megan E. Schmidt[*], **Steven M. Varga**[*,†,‡]

[*]Interdisciplinary Graduate Program in Immunology, University of Iowa, Iowa City, IA 52242

[†]Department of Microbiology and Immunology, University of Iowa, Iowa City, IA 52242

[‡]Department of Pathology, University of Iowa, Iowa City, IA 52242

Abstract

Respiratory syncytial virus (RSV) is the most common cause of lower respiratory tract infection and hospitalization in infants. It is well-established that both $CD4^+$ and $CD8^+$ T cells are critical for mediating viral clearance but also contribute to the induction of immunopathology following RSV infection. C57BL/6 mice are often utilized to study T cell responses following RSV infection given the wide variety of genetically modified animals available. To date, few RSV-derived $CD4^+$ and $CD8^+$ T cell epitopes have been identified in C57BL/6 mice. Utilizing an overlapping peptide library spanning the entire RSV proteome, intracellular cytokine staining for IFN-γ was performed to identify novel $CD4^+$ and $CD8^+$ T cell epitopes in C57BL/6 mice. We identified two novel $CD4^+$ T cell epitopes and three novel $CD8^+$ T cell epitopes located within multiple RSV proteins. Additionally, we characterized the newly described T cell epitopes by determining their TCR Vβ expression profiles and MHC-restriction. Overall, the novel RSV-derived $CD4^+$ and $CD8^+$ T cell epitopes identified in C57BL/6 mice will aid in future studies of RSV-specific T cell responses.

Introduction

Respiratory syncytial virus (RSV) is the leading cause of lower respiratory tract infection in infants and young children (1). RSV represents a substantial healthcare burden worldwide, causing approximately three-four million hospitalizations and 200,000 deaths annually (1). However, despite the immense burden of RSV-associated disease, there remains no licensed RSV vaccine. The peak of disease following RSV infection coincides with the onset of the host immune response, including the expansion of RSV-specific T cells (2). Studies in mouse models of RSV infection have clearly established that both $CD4^+$ and $CD8^+$ T cells contribute to RSV-associated disease, despite their vital role in mediating viral clearance (3). T cells have also been associated with enhanced viral control and exacerbated disease following RSV infection in humans (4–7). Therefore, both $CD4^+$ and $CD8^+$ T cells play a critical role in determining the severity of disease during RSV infection in both mice and humans.

Address correspondence and reprint requests to: Dr. Steven M. Varga, 51 Newton Road, 3-532 Bowen Science Building, University of Iowa, Iowa City, IA 52242. steven-varga@uiowa.edu.

C57BL/6 mice are susceptible to RSV infection and are often utilized as an animal model for RSV. Given the wide variety of genetically modified mice that are available on the H-2^b genetic background, C57BL/6 mice are frequently used for studying RSV-specific T cells. Several T cell epitopes have been defined in C57BL/6 mice using prediction algorithms and peptide library screening techniques. Three RSV-derived $CD4^+$ T cell epitopes in the RSV matrix (M), attachment glycoprotein (G), and M2–1 proteins ($G_{168–185}$, $M_{209–223}$, and $M2–1_{26–39}$) have been previously described (8–10). $CD8^+$ T cell epitopes against RSV in C57BL/6 mice have also been identified, including the immunodominant epitope within the RSV M protein, $M_{187–195}$ (11). Several additional subdominant $CD8^+$ T cell epitopes have also been described within the RSV nucleoprotein (N), fusion glycoprotein (F), and G proteins ($N_{57–64}$, $N_{360–368}$, $F_{250–258}$, $F_{433–442}$, and $G_{177–188}$). Therefore, known $CD4^+$ or $CD8^+$ T cell epitopes in C57BL/6 mice are located within the RSV M, G, N, F, and M2–1 proteins. However, the remaining RSV proteins lack defined RSV-derived T cell epitopes in C57BL/6 mice.

In this study, we utilized a peptide library spanning the entire RSV proteome to identify novel RSV-derived $CD4^+$ and $CD8^+$ T cell epitopes in C57BL/6 mice. We discovered two novel $CD4^+$ T cell epitopes and three novel $CD8^+$ T cell epitopes against RSV in C57BL/6 mice. Additionally, we defined the TCR Vβ profiles and the MHC-restriction of the newly identified T cell epitopes. Overall, the discovery of these novel $CD4^+$ and $CD8^+$ T cell epitopes will provide valuable tools for the study of RSV-specific T cell responses in C57BL/6 mice.

Materials and Methods

Mice and infection

Female C57BL/6 mice between 6–8 weeks of age were purchased from National Cancer Institute (Frederick, MD). The A2 strain of RSV (RSV-A2) was a gift from Dr. Barney Graham (National Institutes of Health, Bethesda, MD) and was propagated on HEp-2 cells (ATCC). Mice were infected intranasally with $1.6–2.5 \times 10^6$ PFU RSV-A2. The A/Puerto Rico/8/34 strain of influenza (IAV) was a gift from Dr. Kevin Legge (University of Iowa). Mice were infected intranasally with a 0.1 LD_{50} dose of IAV. All experimental procedures utilizing mice were approved by the University of Iowa Animal Care and Use Committee. The experiments were performed under strict accordance to the Office of Laboratory Animal Welfare guidelines and the PHS Policy on Humane Care and Use of Laboratory Animals.

Peptides and epitope mapping

A peptide library spanning the entire RSV-A2 proteome consisting of 889 peptides (15-mer overlapping every 10 amino acids) was utilized to screen for novel T cell epitopes (Mimotopes Pty. Ltd., Roseville, MN). For initial screening, the software program *Deconvolute This* (Version 2.0; courtesy of Dr. Mario Roederer, Vaccine Research Center, NIAID, NIH) was used to generate a set of peptide pools, such that each library peptide was represented in two unique pools of 10 peptides each (12). *Deconvolute This* software was utilized to identify potential peptides contributing to a positive response, which was defined as being ≥ 3-SD over the average of no peptide controls in both unique pools in both of two

independent experiments. The identified potential epitopes were screened individually, and peptides eliciting a response ≥ 3-SD above the average of no peptide controls in both of two independent experiments were considered confirmed epitopes. $CD8^+$ T cell minimal core epitopes were predicted using the immune epitope database (IEDB) analysis resource consensus tool (13), which combines predictions from artificial neural networks, also known as NetMHC (14–16), stabilized matrix method (17), and comblib (18). 9-mer peptides of the predicted $CD8^+$ T cell minimal core epitopes were synthesized for epitope confirmation (Biosynthesis, Lewisville, TX).

Ex vivo peptide stimulation

Lungs were harvested from RSV-infected mice on day 8 post-infection (p.i.), and single-cell suspensions were generated as previously described (19, 20). Cells were stimulated with either peptide pools or individual peptides at 1 μM per peptide for 5 hrs at 37°C in the presence of 10 μg/ml brefeldin A (BFA; Sigma-Aldrich) in 10% FCS-supplemented RPMI. In certain experiments, the peptide concentrations were titrated from 10 μM to 0.000001 μM per well. No peptide controls were incubated with 10 μg/ml BFA in 10% FCS-supplemented RPMI in the absence of peptides for 5 hrs at 37°C.

MHC class I restriction assay

Parent P815 cells not expressing $H\text{-}2^b$ MHC class I molecules and P815 cells stably expressing $H\text{-}2D^b$ or $H\text{-}2K^b$ MHC class I molecules were a gift from Dr. John Harty (University of Iowa). P815 cell lines were pulsed with 1 μM peptide at 37°C for 1 hour and washed twice. $CD8^+$ T cells were isolated from the lungs using anti-CD8a microbeads (Miltenyi Biotec, Auburn, CA) and pre-sorted via positive selection on a MidiMACS separator (Miltenyi Biotec). Positively selected cells were stained extracellularly with a monoclonal antibody specific to CD8 (clone 53–6.7) and purified populations of $CD8^+$ T cells were sorted using a FACSAria (BD Biosciences). Sort-purified $CD8^+$ T cells were stimulated with either peptide-pulsed P815 cells or unpulsed P815 cells at a 2:1 effector-to-stimulator ratio for 5 hrs at 37°C in the presence of 10 μg/ml BFA in 10% FCS-supplemented RPMI.

Flow cytometry analysis

Following stimulation, cells were stained extracellularly with monoclonal antibodies specific to CD90.2 (BioLegend; clone 53–2.1), CD4 (clone RM4–5), CD8 (clone 53–6.7), and CD11a (clone M17/4) in FACS buffer (PBS, 2% FCS, 0.02% sodium azide) for 30 mins at 4°C. For TCR Vβ usage analysis, cells were stained with one antibody from a 15 antibody TCR Vβ staining panel (BD Biosciences). Background staining was detected using fluorescence minus one controls and subtracted from the frequency of $V\beta^+$ T cells. After extracellular staining, cells were fixed using 1-step Fix/Lyse Solution for 10 mins at room temperature (eBioscience). Cells were stained intracellularly for IFN-γ (clone XMG1.2) in FACS buffer containing 0.5% saponin (Sigma-Aldrich) for 30 mins at 4°C. All antibodies were purchased from eBioscience unless otherwise indicated. Samples were run on a BD LSRFortessa and analyzed using FlowJo software (Tree Star, Inc., Ashland, OR). Cell types were gated as follows: $CD4^+$ T cells ($CD90.2^+CD4^+$) and $CD8^+$ T cells ($CD90.2^+CD8^+$).

Statistical analysis

All statistical analyses were performed using Prism software (GraphPad Software, San Diego, CA). Data were evaluated using Student's *t* test for two groups or two-way ANOVA with Tukey's post-test for more than two groups as indicated in the figure legends to determine if there was a statistical significance of at least $\alpha = 0.05$.

Results

Identification of candidate CD4$^+$ T cell epitopes

An 889 15-mer peptide library, overlapping every 10 amino acids, spanning the entire RSV proteome was utilized to identify novel RSV T cell epitopes in C57BL/6 mice (21). To increase assay efficiency and reduce the number of animals required, library peptides were divided into peptide pools using *Deconvolute This* software for initial screening (12). Pools containing 10 peptides were created such that each library peptide was included within two unique pools for 179 total pools. Lung cells from day 8 RSV-infected C57BL/6 mice were stimulated with the peptide pools, and CD4$^+$ T cell reactivity was measured by intracellular cytokine staining (ICS) for IFN-γ. A positive pool was defined as having results ≥ 3-SD above the average of no peptide controls.

To validate our experimental approach, we determined whether the previously defined CD4$^+$ T cell epitopes in C57BL/6 mice, $M_{209–223}$ and M2–$1_{26–39}$, and pools containing their corresponding peptides within the peptide library elicited a positive response (9). Both $M_{209–223}$ and M2–$1_{26–39}$ CD4$^+$ T cell epitopes stimulated responses exceeding the 3-SD threshold (Fig. 1A). Importantly, all pools containing their corresponding library peptides, $M_{211–225}$ (pools 65 and 144) and M2–$1_{26–40}$ (pools 36 and 150), also produced positive responses above the 3-SD threshold (Fig. 1). These results indicate that the peptide pooling approach is sufficient to identify potential CD4$^+$ T cell epitopes. Stimulation with the 179 peptide pools resulted in a total of 17 positive pools exceeding the 3-SD threshold for positivity (Fig. 1B). Individual peptides potentially contributing to a positive response were detected using the *Deconvolute This* software and defined as peptides contained in two positive pools in both of two independent experiments. A total of 16 individual peptides within the pools were identified as candidate CD4$^+$ T cell epitopes for further analysis.

Confirmation of novel CD4$^+$ T cell epitopes

To confirm the CD4$^+$ T cell epitope candidates, lung cells from RSV-infected C57BL/6 mice were stimulated with each candidate peptide individually and assessed for IFN-γ production by ICS. A total of four candidate peptides elicited a frequency of IFN-γ^+ CD4$^+$ T cells that exceeded the 3-SD threshold for positivity (Fig. 2A). Two of the identified CD4$^+$ T cell epitopes, $M_{211–225}$ and M2–$1_{26–40}$, contain the previously defined epitopes $M_{209–223}$ and M2–$1_{26–39}$. Two novel RSV CD4$^+$ T cell epitopes in C57BL/6 mice were identified: $M_{166–180}$ and $N_{346–360}$. Importantly, CD4$^+$ T cells harvested from either naive or IAV-infected C57BL/6 mice did not produce IFN-γ above background levels following stimulation with $M_{166–180}$ and $N_{346–360}$ peptides (Fig. 2B, 2C). These results confirm that $M_{166–180}$ and $N_{346–360}$ are true RSV-derived CD4$^+$ T cell epitopes, as cross-recognition by non-RSV-specific CD4$^+$ T cells did not occur. Both $M_{166–180}$ and $N_{346–360}$ epitopes are H2-

I-A^b MHC class II-restricted, as C57BL/6 mice lack expression of the mature H2-I-E^b MHC class II molecule (22).

Because we have previously found that $CD4^+$ T cells that recognize the RSV I-E^d-restricted T cell epitope $G_{183–195}$ predominately express TCR Vβ14, we evaluated the $CD4^+$ T cell repertoire of the novel $CD4^+$ T cell epitopes by staining with a panel of TCR Vβ-specific antibodies (23, 24). As expected, lung $CD4^+$ T cells from naive C57BL/6 mice exhibit a polyclonal TCR repertoire (Fig. 3A). Vβ8.1/8.2 is the TCR Vβ chain most highly expressed by naive $CD4^+$ T cells. Vβ4, Vβ6, and Vβ14 are represented at comparable levels with smaller contributions from the other Vβ chains. Similar to naive $CD4^+$ T cells, $M_{166–180}$-specific $CD4^+$ T cells exhibit a polyclonal TCR repertoire in which Vβ8.1/8.2 is most highly represented, followed by smaller frequencies of Vβ3-, Vβ6-, and Vβ8.3-expressing cells (Fig. 3B). Vβ8.1/8.2 is also highly represented in the $N_{346–360}$-specific $CD4^+$ T cell TCR repertoire, followed closely by a population of cells expressing Vβ6 (Fig. 3C). These results are similar to the TCR repertoires of previously defined epitopes $M_{209–223}$ and $M2–1_{26–39}$, which are also highly represented by Vβ8.1/8.2-expressing cells (25).

Identification of candidate $CD8^+$ T cell epitopes

We used a similar strategy as outlined for the $CD4^+$ T cells to identify candidate RSV $CD8^+$ T cell epitopes in C57BL/6 mice. Similar to the $CD4^+$ T cell epitope screen, positive pools were defined as those having $CD8^+$ T cell IFN-γ responses ≥ 3-SD above the average of no peptide controls. To verify the approach for the identification of $CD8^+$ T cell epitopes, we evaluated whether pools containing the peptides encompassing the previously defined immunodominant $CD8^+$ T cell epitope in C57BL/6 mice, $M_{187–195}$, elicited positive responses (11). As expected, $M_{187–195}$ stimulated robust $CD8^+$ T cell responses well above the 3-SD threshold (Fig. 4A). Similarly, all pools containing its corresponding library peptides, $M_{181–195}$ (pools 65 and 116) and $M_{186–200}$ (pools 5 and 108), exhibited positive IFN-γ responses above the 3-SD threshold (Fig. 4). Stimulation with the 179 peptide pools resulted in a total of 127 positive pools meeting the 3-SD threshold for positivity, much greater than the number of positive responses observed during the $CD4^+$ T cell epitope screen (Fig. 4B). Following this initial screening, *Deconvolute This* software identified 510 individual peptides potentially contributing to the positive responses. To reduce the overall number of peptides requiring individual testing, a second peptide pool screen (204 total pools of 5 peptides each) for $CD8^+$ T cell reactivity was performed yielding 155 positive pools (data not shown). Deconvolution of this response identified a total of 352 candidate $CD8^+$ T cell epitopes for individual screening.

Confirmation and evaluation of novel $CD8^+$ T cell epitopes

To confirm the $CD8^+$ T cell epitope candidates, IFN-γ production following stimulation of lung cells with each of the 352 candidate peptides individually was evaluated by ICS. A total of 72 candidate peptides elicited a positive IFN-γ response above the 3-SD threshold in both of two individual experiments (Fig. 5A, Supplemental Table 1). Included within the positive candidate peptides are three peptides containing either the entire or partial peptide sequence of the previously defined $CD8^+$ T cell epitope $M_{187–195}$ (Fig. 5, Supplemental Table 1). In total, 69 candidate peptides were identified as potential novel $CD8^+$ T cell epitopes,

although the overall number of $CD8^+$ T cell epitopes is likely fewer given the overlapping nature of the peptide library utilized (Supplementary Table 1).

Of the 69 potential novel $CD8^+$ T cell epitopes identified, we selected three $CD8^+$ T cell epitopes to confirm and utilize for further study: $NS1_{61–75}$, $M_{111–125}$, and $L_{2021–2035}$ (Fig. 5). We selected $NS1_{61–75}$ and $L_{2021–2035}$ because no H-2^b-restricted $CD8^+$ T cell epitopes are currently known within the RSV NS1 and L proteins. $M_{111–125}$ was chosen to identify a potential subdominant $CD8^+$ T cell epitope within the RSV M protein to evaluate in addition to the immunodominant $CD8^+$ T cell epitope, $M_{187–195}$. To confirm these novel $CD8^+$ T cell epitopes, we first utilized cell lines expressing H-$2D^b$ and H-$2K^b$ MHC class I molecules to determine their MHC class I-restriction. Sort-purified $CD8^+$ T cells isolated from the lungs of RSV-infected C57BL/6 mice were stimulated with peptide-pulsed parent P815 cells or P815 cells expressing either H-$2D^b$ or H-$2K^b$ and assessed for IFN-γ production by ICS. As previously described, the $M_{187–195}$ $CD8^+$ T cell epitope is H-$2D^b$ MHC class I-restricted (Fig. 6A) (11). Similarly, the three newly identified epitopes $NS1_{61–75}$, $M_{111–125}$, and $L_{2021–2035}$ are all also H-$2D^b$ MHC class I-restricted (Fig. 6A). Importantly, $CD8^+$ T cells did not produce IFN-γ following stimulation with P815 cells that were not pulsed with peptides, confirming that they are responding specifically to the RSV-derived peptides bound to the H-$2D^b$ MHC class I molecule (Fig. 6A). After determining the MHC restriction of the newly identified $CD8^+$ T cell epitopes, we predicted their minimal core $CD8^+$ T cell epitope sequence using the IEDB analysis resource (13). The IEDB resource identified the minimal 9-mer sequences with the highest percentile rank of $NS1_{61–75}$, $M_{111–125}$, and $L_{2021–2035}$ epitopes to be $NS1_{65–73}$ (ICPNNNIVV), $M_{112–120}$ (IKACSLTCL), and $L_{2021–2029}$ (NVVQNAKLI), respectively. Peptides for the three core minimal epitopes were synthesized and used to stimulate lung cells for confirmation. $NS1_{65–73}$, $M_{112–120}$, and $L_{2021–2029}$ minimal core epitopes all elicited strong IFN-γ production by $CD8^+$ T cells (Fig. 6B). Additionally, the vast majority of IFN-γ^+ $CD8^+$ T cells express high levels of the integrin CD11a after peptide stimulation, indicating that they are antigen-experienced cells (Fig. 6B) (26). To confirm that the 9-mer minimal core epitope sequences were recognized at enhanced or similar levels as the 15-mer library peptides, the peptide concentration used for stimulation was titrated from 10^1 to 10^{-6} μM (Fig. 6C). $NS1_{65–73}$ and $L_{2021–2029}$ stimulation exhibited increased IFN-γ^+ $CD8^+$ T cells compared to stimulation with their 15-mer peptide library counterparts down to 10^{-4} μM, indicating that they are strongly recognized (Fig. 6C). In contrast, $M_{112–120}$ stimulation resulted in similar levels of IFN-γ^+ $CD8^+$ T cells as stimulation with its 15-mer peptide library counterpart at all peptide concentrations (Fig. 6C). Three additional peptides within the $M_{111–125}$ 15-mer library peptide sequence were identified by the IEDB resource as having medium-high percentile rankings, $M_{113–121}$, $M_{115–123}$, and $M_{117–125}$, but did not elicit IFN-γ production following stimulation at any peptide concentration (data not shown). Therefore, given the consistent and robust results obtained with $M_{112–120}$, it is highly likely that $M_{112–120}$ is the confirmed minimal $CD8^+$ T cell epitope within the $M_{111–125}$ sequence. Similar to the novel $CD4^+$ T cell epitopes, stimulation with $NS1_{65–73}$, $M_{112–120}$, and $L_{2021–2029}$ did not induce IFN-γ production above background levels by $CD8^+$ T cells harvested from either naive or IAV-infected C57BL/6 mice, confirming that they are bona-fide RSV-derived $CD8^+$ T cell epitopes (Fig. 6D, 6E).

We also determined the epitope-specific $CD8^+$ T cell repertoire of the novel $CD8^+$ T cell epitopes by staining with a panel of TCR Vβ-specific antibodies. Similar to naive $CD4^+$ T cells, $CD8^+$ T cells from the lungs of naive C57BL/6 mice exhibit a polyclonal TCR repertoire in which Vβ8.1/8.2 is most highly expressed, followed closely by Vβ5.1/5.2 (Fig. 7A). Vβ6, Vβ7, Vβ8.3, Vβ10, Vβ11, and Vβ13 are also well-represented in naive $CD8^+$ T cells within the lung. $NS1_{65–73}$-specific $CD8^+$ T cells also express a polyclonal TCR repertoire, but the expression of individual Vβ chains are highly variable between mice, unlike in naive $CD8^+$ T cells (Fig. 7B). Both $M_{112–120}$ and $L_{2021–2029}$ exhibit highly skewed $CD8^+$ T cell repertoires that are dominated by Vβ9 with smaller contributions made by Vβ6 and Vβ8.1/8.2 for $M_{112–120}$ and Vβ13 for $L_{2021–2029}$ (Fig. 7C–D). The oligoclonal TCR repertoires of $M_{112–120}$ and $L_{2021–2029}$ are similar to that of the previously described $CD8^+$ T cell epitope $M_{187–195}$, which also predominately expresses Vβ9 following RSV infection (27).

In addition to the $NS1_{65–73}$, $M_{112–120}$, and $L_{2021–2029}$ $CD8^+$ T cell epitopes identified, we attempted to confirm novel $CD8^+$ T cell epitopes within eight additional RSV library peptides that elicited positive IFN-γ responses in the individual candidate peptide screen (Fig. 5A). Four 15-mer library peptides within the RSV M protein were evaluated for potential $CD8^+$ T cell epitopes, three of which exhibited large IFN-γ production (>3%) in the candidate screen (Fig. 5A). Additionally, one 15-mer peptide within each of the RSV NS1, NS2, P, and L proteins were also tested for $CD8^+$ T cell epitopes. However, we were not able to confirm RSV-derived $CD8^+$ T cell epitopes within these other library peptides, as stimulation with predicted 9-mer amino acid sequences resulted in low IFN-γ production similar to background levels (data not shown). Alternatively, stimulation with multiple predicted 9-mer peptide sequences elicited IFN-γ production by $CD8^+$ T cells above background levels. However, the responses observed were either significantly reduced compared to stimulation with the 15-mer library peptides or titration of the peptide concentration resulted in an immediate decline in IFN-γ production that was similar to background levels (data not shown). These results may help explain the large number of positive candidate peptides identified in the individual $CD8^+$ T cell epitope screen (Fig. 5A). Therefore, while additional novel $CD8^+$ T cell epitopes are likely present within the library peptides that were positive in the individual screen, only $NS1_{65–73}$, $M_{112–120}$, and $L_{2021–2029}$ have been confirmed to date.

Discussion

In this study, we utilized an overlapping peptide library spanning the entire RSV proteome to identify novel RSV-derived $CD4^+$ and $CD8^+$ T cell epitopes in C57BL/6 mice. The initial screening was performed using a peptide pooling approach, as has been described in the screening of T cell epitopes for a variety of other viruses (28–32). The peptide pooling approach was validated by confirming that pools containing library peptides that correspond to previously defined $CD4^+$ and $CD8^+$ T cell epitopes exhibited IFN-γ production above the 3-SD threshold for positivity. Library peptides containing the most widely used $CD4^+$ T cell epitopes $M_{209–223}$ and $M2–1_{26–39}$ and the immunodominant $CD8^+$ T cell epitope $M_{187–195}$ elicited positive responses, validating this experimental approach. In contrast, pools containing library peptides that represented the amino acid sequences of less widely utilized

T cell epitopes against RSV in C57BL/6 mice did not produce positive responses, including the $CD4^+$ T cell epitope $G_{168–185}$ and the $CD8^+$ T cell epitopes $N_{57–64}$, $N_{360–368}$, $F_{250–258}$, $F_{433–442}$, and $G_{177–188}$. The differential ability for defined $CD4^+$ and $CD8^+$ T cell epitopes to induce positive IFN-γ responses within peptide pools may be due to a variety of factors. Given that there are multiple peptides in each pool, it is possible that peptides not corresponding to RSV T cell epitopes bind with a high affinity to the MHC molecule, preventing other peptides within the pool from attaching to the MHC molecule's peptide binding groove. Alternatively, the 15-mer peptides utilized may not be the optimal size for eliciting a T cell response *in vitro*. We have previously shown that the use of 17-mer peptides induced an increased frequency of responding $CD4^+$ T cells from RSV-infected BALB/c mice than 15-mer peptides (21). Therefore, it is likely that 17-mer peptides may also induce IFN-γ production from C57BL/6 $CD4^+$ T cells more optimally, which may explain why the $G_{168–185}$ $CD4^+$ T cell epitope was negative in our initial screening. Additionally, the 15-mer peptides may not always be cleaved in the correct place to produce the proper amino acid sequence corresponding to a $CD8^+$ T cell epitope that is typically 8–10 amino acids in length. Thus, the peptide library approach we have used here is likely an underestimate of the number of total T cell epitopes.

By screening individual library peptides, we identified two novel RSV-derived $CD4^+$ T cell epitopes in C57BL/6 mice: $M_{166–180}$ and $N_{346–360}$. $M_{166–180}$ provides an additional $CD4^+$ T cell epitope within the RSV M protein that is of similar size to the previously defined $M_{209–223}$ $CD4^+$ T cell epitope. $N_{346–360}$ represents the first $CD4^+$ T cell epitope in C57BL/6 mice within the RSV N protein. Additionally, we confirmed three novel $CD8^+$ T cell epitopes against RSV in C57BL/6 mice: $NS1_{65–73}$, $M_{112–120}$, and $L_{2021–2029}$. $NS1_{65–73}$ is the first RSV-derived T cell epitope to be described within the RSV NS1 protein in any mouse model. NS1 and NS2 are the first and most abundant viral gene products synthesized following RSV infection (33). Given the abundance of NS1 and NS2 proteins within a host cell, it is interesting that there is only a single defined murine T cell epitope within NS1 and none within NS2. Similarly, $L_{2021–2029}$ is the first murine $CD8^+$ T cell epitope identified within the RSV L protein. Lastly, $M_{112–120}$ provides an additional subdominant $CD8^+$ T cell epitope in C57BL/6 mice within the RSV M protein to study alongside the immunodominant $CD8^+$ T cell epitope, $M_{187–195}$.

In addition to confirming the novel $CD4^+$ and $CD8^+$ T cell epitopes, we characterized their TCR Vβ expression profiles. Lung $CD4^+$ T cells from naive C57BL/6 mice express a polyclonal TCR Vβ repertoire in which Vβ8.1/8.2 is the most highly expressed. Similar to the naive $CD4^+$ T cell repertoire, the previously defined $CD4^+$ T cell epitopes $M_{209–223}$ and $M2–1_{26–39}$ exhibit dominant responses by cells expressing Vβ8.1/8.2 (25). The novel $CD4^+$ T cell epitopes $M_{166–180}$ and $N_{346–360}$ also exhibit polyclonal TCR Vβ repertoires in which Vβ8.1/8.2 is the most highly represented. Overall, RSV infection results in the expansion of $CD4^+$ T cells of multiple specificities that predominately express TCR Vβ8.1/8.2. This is in contrast to the Vβ repertoire of the I-E^d-restricted T cell epitope $G_{183–195}$ in BALB/c mice, which predominately express TCR Vβ14 (23, 24). The naive $CD8^+$ T cell Vβ repertoire in the lung of C57BL/6 mice is also polyclonal with Vβ8.1/8.2 and Vβ5.1/5.2 expressed with the highest frequency. This is a similar pattern to what was previously observed on splenic naive $CD8^+$ T cells in C57BL/6 mice (27). In contrast to the C57BL/6 $CD4^+$ T cell epitopes

which highly express Vβ8.1/8.2, Vβ9 is most highly represented on $CD8^+$ T cells specific to the previously described $CD8^+$ T cell epitope $M_{187–195}$ (27). Similarly, the TCR Vβ usage of $M_{112–120}$ and $L_{2021–2029}$ $CD8^+$ T cell epitopes is dominated by Vβ9 with very small frequencies of epitope-specific $CD8^+$ T cells expressing other TCR Vβ chains. In contrast, $NS1_{65–73}$-specific $CD8^+$ T cells exhibit a polyclonal Vβ repertoire that is highly variable between mice. It is particularly interesting that the Vβ repertoire for $NS1_{65–73}$-specific $CD8^+$ T cells is highly variable, in contrast to other RSV-derived $CD8^+$ T cell epitopes which do not exhibit TCR Vβ repertoire variability between individual mice (Figure 7) (27, 34). It is possible that the precursor frequency of $NS1_{65–73}$-specific $CD8^+$ T cells may not be identical between individual C57BL/6 mice. Alternatively, the proliferation capacity of certain $NS1_{65–73}$-specific $CD8^+$ T clones may be different between individual C57BL/6 mice. The mechanism underlying the variability of the $NS1_{65–73}$-specific $CD8^+$ T cell Vβ repertoire is an interesting topic for future study. Overall, the TCR Vβ repertoire of RSV-specific T cells tends to skew towards Vβ8.1/8.2 for $CD4^+$ T cells and Vβ9 for $CD8^+$ T cells, with the exception of the $CD8^+$ T cell epitope $NS1_{65–73}$.

In summary, we have identified two novel RSV-derived $CD4^+$ T cell epitopes, $M_{166–180}$ and $N_{346–360}$, and three novel RSV-derived $CD8^+$ T cell epitopes, $NS1_{65–73}$, $M_{112–120}$, and $L_{2021–2029}$, in C57BL/6 mice. We have also characterized the TCR Vβ expression profile as well as the MHC-restriction of each new T cell epitope described. In addition to utilizing these epitopes to perform *ex vivo* peptide stimulation, the characterization of their TCR Vβ expression profiles and MHC-restriction provides information that could aid in the generation of transgenic T cell lines and peptide-MHC tetramers to probe antigen-specific responses following RSV infection. While these novel T cell epitopes will be useful in future studies of C57BL/6 mice, they will also be important for the study of T cells in the CB6F1 model, a cross between C57BL/6 and BALB/c mice, which is also frequently used as a murine model for RSV infection (27, 34–40). Overall, the discovery of these novel T cell epitopes in C57BL/6 mice will provide valuable tools for further understanding RSV-specific T cell responses.

Supplementary Material

Refer to Web version on PubMed Central for supplementary material.

Acknowledgments

We thank Stacey Hartwig for excellent technical assistance and Justin Fishbaugh, Heath Vignes, and Michael Shey of the University of Iowa Flow Cytometry Facility for assistance with cell sorting.

Some of the data presented herein were obtained at the Flow Cytometry Facility, which is a Carver College of Medicine / Holden Comprehensive Cancer Center core research facility at the University of Iowa. The facility is funded through user fees and the generous financial support of the Carver College of Medicine, Holden Comprehensive Cancer Center, Iowa City Veteran's Administration Medical Center, and the National Center for Research Resources of the National Institutes of Health under Award Number 1 S10 OD016199-01A1. This work was supported by the Department of Microbiology and Immunology at the University of Iowa (to SMV) and the National Institute of Allergy and Infectious Diseases of the National Institutes of Health under Award Numbers R01AI124093 (to SMV) and T32AI007485 (to MES). The content is solely the responsibility of the authors and does not necessarily represent the official views of the National Institutes of Health.

Abbreviations used in this article:

RSV	respiratory syncytial virus
IAV	influenza
IEDB	immune epitope database
p.i.	post-infection
BFA	brefeldin A
ICS	intracellular cytokine staining

References

1. Nair H, Nokes DJ, Gessner BD, Dherani M, Madhi SA, Singleton RJ, O'Brien KL, Roca A, Wright PF, Bruce N, Chandran A, Theodoratou E, Sutanto A, Sedyaningsih ER, Ngama M, Munywoki PK, Kartasasmita C, Simoes EA, Rudan I, Weber MW, and Campbell H. 2010 Global burden of acute lower respiratory infections due to respiratory syncytial virus in young children: a systematic review and meta-analysis. Lancet 375: 1545–1555. [PubMed: 20399493]
2. Openshaw PJ, and Tregoning JS. 2005 Immune responses and disease enhancement during respiratory syncytial virus infection. Clin Microbiol Rev 18: 541–555. [PubMed: 16020689]
3. Graham BS, Bunton LA, Wright PF, and Karzon DT. 1991 Role of T lymphocyte subsets in the pathogenesis of primary infection and rechallenge with respiratory syncytial virus in mice. J Clin Invest 88: 1026–1033. [PubMed: 1909350]
4. El Saleeby CM, Suzich J, Conley ME, and DeVincenzo JP. 2004 Quantitative effects of palivizumab and donor-derived T cells on chronic respiratory syncytial virus infection, lung disease, and fusion glycoprotein amino acid sequences in a patient before and after bone marrow transplantation. Clin Infect Dis 39: e17–20. [PubMed: 15307047]
5. Fishaut M, Tubergen D, and McIntosh K. 1980 Cellular response to respiratory viruses with particular reference to children with disorders of cell-mediated immunity. J Pediatr 96: 179–186. [PubMed: 6243354]
6. Hall CB, Powell KR, MacDonald NE, Gala CL, Menegus ME, Suffin SC, and Cohen HJ. 1986 Respiratory syncytial viral infection in children with compromised immune function. N Engl J Med 315: 77–81. [PubMed: 3724802]
7. Jozwik A, Habibi MS, Paras A, Zhu J, Guvenel A, Dhariwal J, Almond M, Wong EH, Sykes A, Maybeno M, Del Rosario J, Trujillo-Torralbo MB, Mallia P, Sidney J, Peters B, Kon OM, Sette A, Johnston SL, Openshaw PJ, and Chiu C. 2015 RSV-specific airway resident memory CD8+ T cells and differential disease severity after experimental human infection. Nat Commun 6: 10224. [PubMed: 26687547]
8. Hancock GE, Tebbey PW, Scheuer CA, Pryharski KS, Heers KM, and LaPierre NA. 2003 Immune responses to the nonglycosylated ectodomain of respiratory syncytial virus attachment glycoprotein mediate pulmonary eosinophilia in inbred strains of mice with different MHC haplotypes. J Med Virol 70: 301–308. [PubMed: 12696122]
9. Liu J, Ruckwardt TJ, Chen M, Johnson TR, and Graham BS. 2009 Characterization of respiratory syncytial virus M- and M2-specific CD4 T cells in a murine model. J Virol 83: 4934–4941. [PubMed: 19264776]
10. Srikiatkhachorn A, Chang W, and Braciale TJ. 1999 Induction of Th-1 and Th-2 responses by respiratory syncytial virus attachment glycoprotein is epitope and major histocompatibility complex independent. J Virol 73: 6590–6597. [PubMed: 10400756]
11. Rutigliano JA, Rock MT, Johnson AK, Crowe JE Jr., and Graham BS. 2005 Identification of an H-2D(b)-restricted CD8+ cytotoxic T lymphocyte epitope in the matrix protein of respiratory syncytial virus. Virology 337: 335–343. [PubMed: 15916793]

12. Roederer M, and Koup RA. 2003 Optimized determination of T cell epitope responses. J Immunol Methods 274: 221–228. [PubMed: 12609547]
13. Vita R, Overton JA, Greenbaum JA, Ponomarenko J, Clark JD, Cantrell JR, Wheeler DK, Gabbard JL, Hix D, Sette A, and Peters B. 2015 The immune epitope database (IEDB) 3.0. Nucleic Acids Res 43: D405–412. [PubMed: 25300482]
14. Andreatta M, and Nielsen M. 2016 Gapped sequence alignment using artificial neural networks: application to the MHC class I system. Bioinformatics 32: 511–517. [PubMed: 26515819]
15. Lundegaard C, Lamberth K, Harndahl M, Buus S, Lund O, and Nielsen M. 2008 NetMHC-3.0: accurate web accessible predictions of human, mouse and monkey MHC class I affinities for peptides of length 8–11. Nucleic Acids Res 36: W509–512. [PubMed: 18463140]
16. Nielsen M, Lundegaard C, Worning P, Lauemoller SL, Lamberth K, Buus S, Brunak S, and Lund O. 2003 Reliable prediction of T-cell epitopes using neural networks with novel sequence representations. Protein Sci 12: 1007–1017. [PubMed: 12717023]
17. Peters B, and Sette A. 2005 Generating quantitative models describing the sequence specificity of biological processes with the stabilized matrix method. BMC Bioinformatics 6: 132. [PubMed: 15927070]
18. Sidney J, Assarsson E, Moore C, Ngo S, Pinilla C, Sette A, and Peters B. 2008 Quantitative peptide binding motifs for 19 human and mouse MHC class I molecules derived using positional scanning combinatorial peptide libraries. Immunome Res 4: 2. [PubMed: 18221540]
19. Fulton RB, Olson MR, and Varga SM. 2008 Regulation of cytokine production by virus-specific CD8 T cells in the lungs. J Virol 82: 7799–7811. [PubMed: 18524828]
20. Weiss KA, Christiaansen AF, Fulton RB, Meyerholz DK, and Varga SM. 2011 Multiple CD4+ T cell subsets produce immunomodulatory IL-10 during respiratory syncytial virus infection. J Immunol 187: 3145–3154. [PubMed: 21844390]
21. McDermott DS, Knudson CJ, and Varga SM. 2014 Determining the breadth of the respiratory syncytial virus-specific T cell response. J Virol 88: 3135–3143. [PubMed: 24371055]
22. Jones PP, Murphy DB, and McDevitt HO. 1981 Variable synthesis and expression of E alpha and Ae (E beta) Ia polypeptide chains in mice of different H-2 haplotypes. Immunogenetics 12: 321–337. [PubMed: 6937437]
23. Varga SM, Wissinger EL, and Braciale TJ. 2000 The attachment (G) glycoprotein of respiratory syncytial virus contains a single immunodominant epitope that elicits both Th1 and Th2 CD4+ T cell responses. J Immunol 165: 6487–6495. [PubMed: 11086089]
24. Varga SM, Wang X, Welsh RM, and Braciale TJ. 2001 Immunopathology in RSV infection is mediated by a discrete oligoclonal subset of antigen-specific CD4(+) T cells. Immunity 15: 637–646. [PubMed: 11672545]
25. Liu J, Cao S, Peppers G, Kim SH, and Graham BS. 2014 Clonotype-specific avidity influences the dynamics and hierarchy of virus-specific regulatory and effector CD4(+) T-cell responses. Eur J Immunol 44: 1058–1068. [PubMed: 24510524]
26. Rai D, Pham NL, Harty JT, and Badovinac VP. 2009 Tracking the total CD8 T cell response to infection reveals substantial discordance in magnitude and kinetics between inbred and outbred hosts. J Immunol 183: 7672–7681. [PubMed: 19933864]
27. Billam P, Bonaparte KL, Liu J, Ruckwardt TJ, Chen M, Ryder AB, Wang R, Dash P, Thomas PG, and Graham BS. 2011 T Cell receptor clonotype influences epitope hierarchy in the CD8+ T cell response to respiratory syncytial virus infection. J Biol Chem 286: 4829–4841. [PubMed: 21118816]
28. Kennedy RB, and Poland GA. 2010 The identification of HLA class II-restricted T cell epitopes to vaccinia virus membrane proteins. Virology 408: 232–240. [PubMed: 20961593]
29. Lee LY, Ha do LA, Simmons C, de Jong MD, Chau NV, Schumacher R, Peng YC, McMichael AJ, Farrar JJ, Smith GL, Townsend AR, Askonas BA, Rowland-Jones S, and Dong T. 2008 Memory T cells established by seasonal human influenza A infection cross-react with avian influenza A (H5N1) in healthy individuals. J Clin Invest 118: 3478–3490. [PubMed: 18802496]
30. Leligdowicz A, Yindom LM, Onyango C, Sarge-Njie R, Alabi A, Cotten M, Vincent T, da Costa C, Aaby P, Jaye A, Dong T, McMichael A, Whittle H, and Rowland-Jones S. 2007 Robust Gag-

specific T cell responses characterize viremia control in HIV-2 infection. J Clin Invest 117: 3067–3074. [PubMed: 17823657]

31. Precopio ML, Butterfield TR, Casazza JP, Little SJ, Richman DD, Koup RA, and Roederer M. 2008 Optimizing peptide matrices for identifying T-cell antigens. Cytometry A 73: 1071–1078. [PubMed: 18781655]
32. Richmond M, McKinnon LR, Kiazyk SA, Wachihi C, Kimani M, Kimani J, Plummer FA, and Ball TB. 2011 Epitope mapping of HIV-specific CD8+ T cell responses by multiple immunological readouts reveals distinct specificities defined by function. J Virol 85: 1275–1286. [PubMed: 21084478]
33. Collins PL, and Wertz GW. 1983 cDNA cloning and transcriptional mapping of nine polyadenylylated RNAs encoded by the genome of human respiratory syncytial virus. Proc Natl Acad Sci U S A 80: 3208–3212. [PubMed: 6190173]
34. Ruckwardt TJ, Malloy AM, Gostick E, Price DA, Dash P, McClaren JL, Thomas PG, and Graham BS. 2011 Neonatal CD8 T-cell hierarchy is distinct from adults and is influenced by intrinsic T cell properties in respiratory syncytial virus infected mice. PLoS Pathog 7: e1002377. [PubMed: 22144888]
35. Liu J, Haddad EK, Marceau J, Morabito KM, Rao SS, Filali-Mouhim A, Sekaly RP, and Graham BS. 2016 A Numerically Subdominant CD8 T Cell Response to Matrix Protein of Respiratory Syncytial Virus Controls Infection with Limited Immunopathology. PLoS Pathog 12: e1005486. [PubMed: 26943673]
36. Malloy AM, Ruckwardt TJ, Morabito KM, Lau-Kilby AW, and Graham BS. 2017 Pulmonary Dendritic Cell Subsets Shape the Respiratory Syncytial Virus-Specific CD8+ T Cell Immunodominance Hierarchy in Neonates. J Immunol 198: 394–403. [PubMed: 27895172]
37. Morabito KM, Erez N, Graham BS, and Ruckwardt TJ. 2016 Phenotype and Hierarchy of Two Transgenic T Cell Lines Targeting the Respiratory Syncytial Virus KdM282–90 Epitope Is Transfer Dose-Dependent. PLoS One 11: e0146781. [PubMed: 26752171]
38. Ruckwardt TJ, Bonaparte KL, Nason MC, and Graham BS. 2009 Regulatory T cells promote early influx of CD8+ T cells in the lungs of respiratory syncytial virus-infected mice and diminish immunodominance disparities. J Virol 83: 3019–3028. [PubMed: 19153229]
39. Ruckwardt TJ, Luongo C, Malloy AM, Liu J, Chen M, Collins PL, and Graham BS. 2010 Responses against a subdominant CD8+ T cell epitope protect against immunopathology caused by a dominant epitope. J Immunol 185: 4673–4680. [PubMed: 20833834]
40. Ruckwardt TJ, Malloy AM, Morabito KM, and Graham BS. 2014 Quantitative and qualitative deficits in neonatal lung-migratory dendritic cells impact the generation of the CD8+ T cell response. PLoS Pathog 10: e1003934. [PubMed: 24550729]

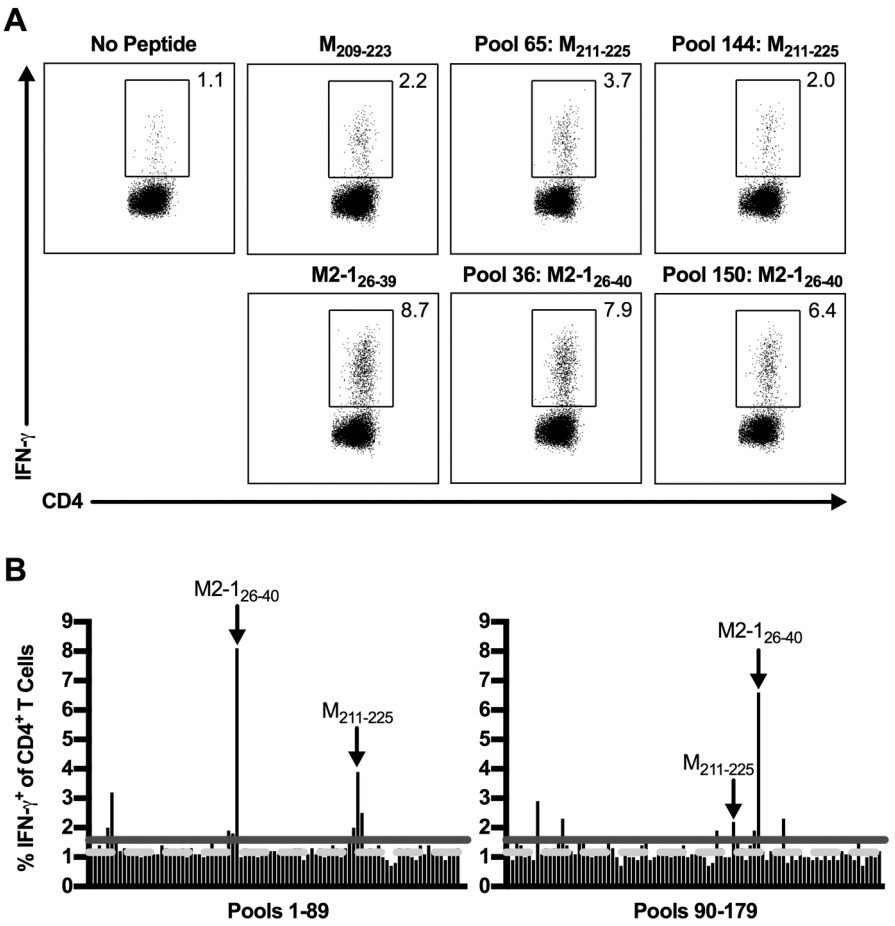

Figure 1. RSV peptide library screen for candidate CD4$^+$ T cell epitopes.

C57BL/6 mice were infected with RSV, and lungs were harvested on day 8 p.i. Lung cells were either incubated with BFA alone or stimulated with a pool containing 10 individual RSV-derived peptides from a peptide library spanning the entire RSV proteome. **(A)** Dot plots show the frequency of IFN-γ^+ CD4$^+$ T cells elicited following peptide stimulation with previously defined CD4$^+$ T cell epitopes, $M_{209–223}$ and $M2–1_{26–39}$, or pools containing their corresponding peptides in the peptide library, $M_{211–225}$ and $M2–1_{26–40}$. **(B)** The frequency of IFN-γ^+ CD4$^+$ T cells induced by peptide stimulation with all peptide pools. The dashed light gray line represents the average of no peptide controls (y=1.16), and the solid dark gray line represents the 3-SD threshold for positivity (y=1.58). Arrows indicate pools containing the previously defined $M_{209–223}$ and $M2–1_{26–39}$ CD4$^+$ T cell epitopes. Data are representative of 1 of 2 experiments with 24 mice pooled per experiment.

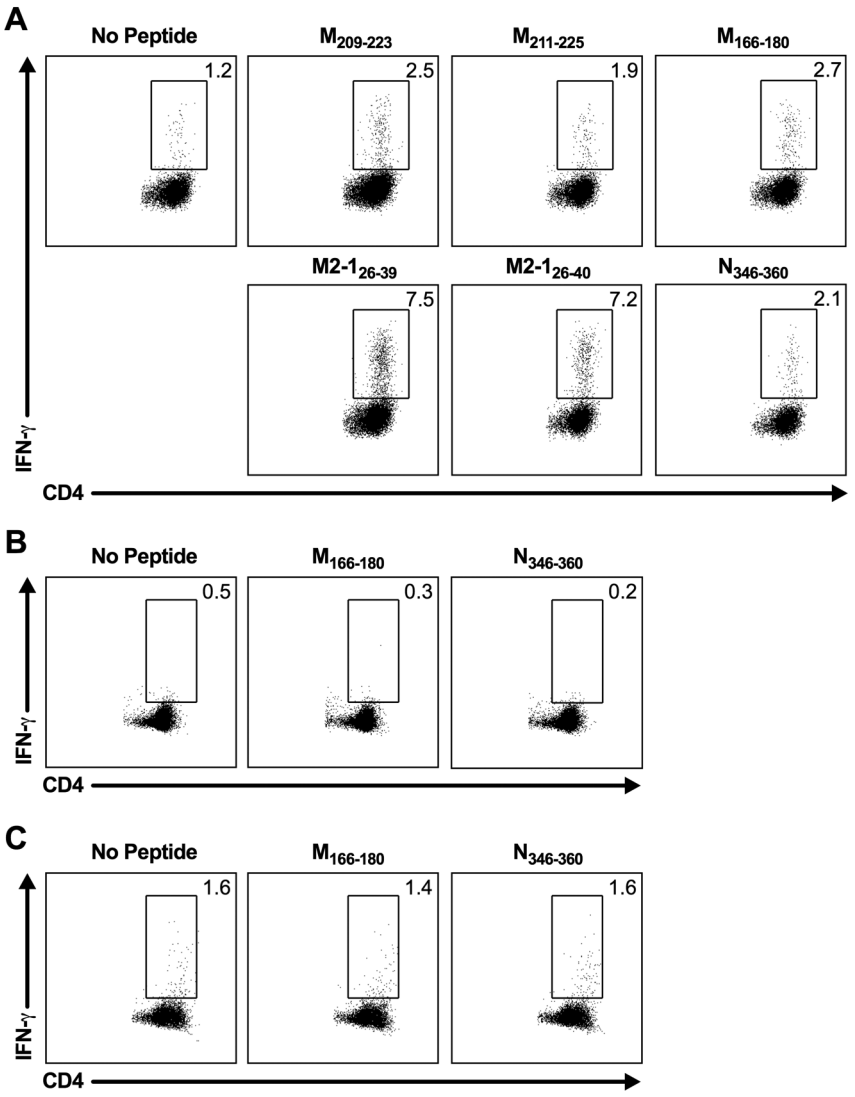

Figure 2. Identification of novel RSV CD4$^+$ T cell epitopes.

(A) C57BL/6 mice were infected with RSV, and lungs were harvested on day 8 p.i. Lung cells were either incubated with BFA alone or stimulated with individual candidate CD4$^+$ T cell epitopes. Dot plots show the frequency of IFN-γ^+ CD4$^+$ T cells elicited by the previously defined CD4$^+$ T cell epitopes, $M_{209–223}$ and $M2–1_{26–39}$, and the individual peptides that are ≥ the 3-SD threshold for positivity, $M_{166–180}$ and $N_{346–360}$. **(B/C)** Lung cells from **(B)** naive C57BL/6 mice or **(C)** day 8 IAV-infected C57BL/6 mice were either incubated with BFA alone or stimulated with $M_{166–180}$ or $N_{346–360}$ peptides and stained intracellularly for IFN-γ. Data are representative of 1 of 2 experiments with **(A)** 30 mice pooled per experiment or **(B/C)** 4 mice per group per experiment.

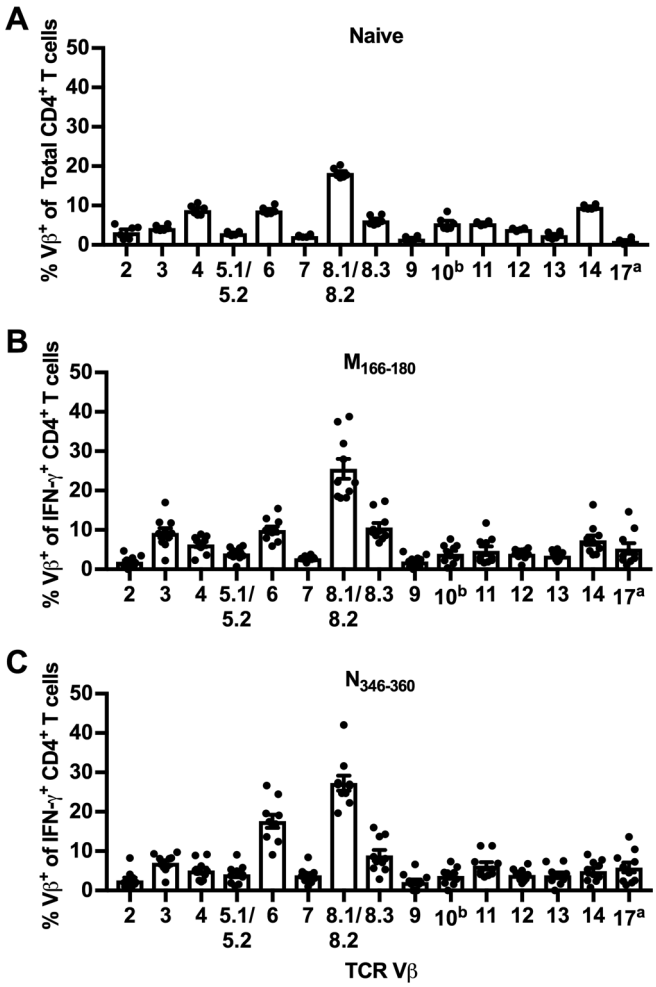

Figure 3. TCR Vβ usage of novel CD4$^+$ T cell epitopes.

(A) TCR Vβ usage of CD4$^+$ T cells in the lungs of naive C57BL/6 mice. **(B/C)** C57BL/6 mice were infected with RSV, and lungs were harvested on day 8 p.i. Lung cells were stimulated with $M_{166–180}$ or $N_{346–360}$ peptides, stained extracellularly with a panel of TCR Vβ-specific antibodies, and stained intracellularly for IFN-γ. Lung cells were gated on IFN-γ$^+$ CD4$^+$ T cells and graphs show the TCR Vβ usage of **(B)** $M_{166–180}$- and **(C)** $N_{346–360}$-specific CD4$^+$ T cells. Data are presented as mean ± SEM of 2–3 independent experiments. Each dot represents an individual mouse (n=6–10).

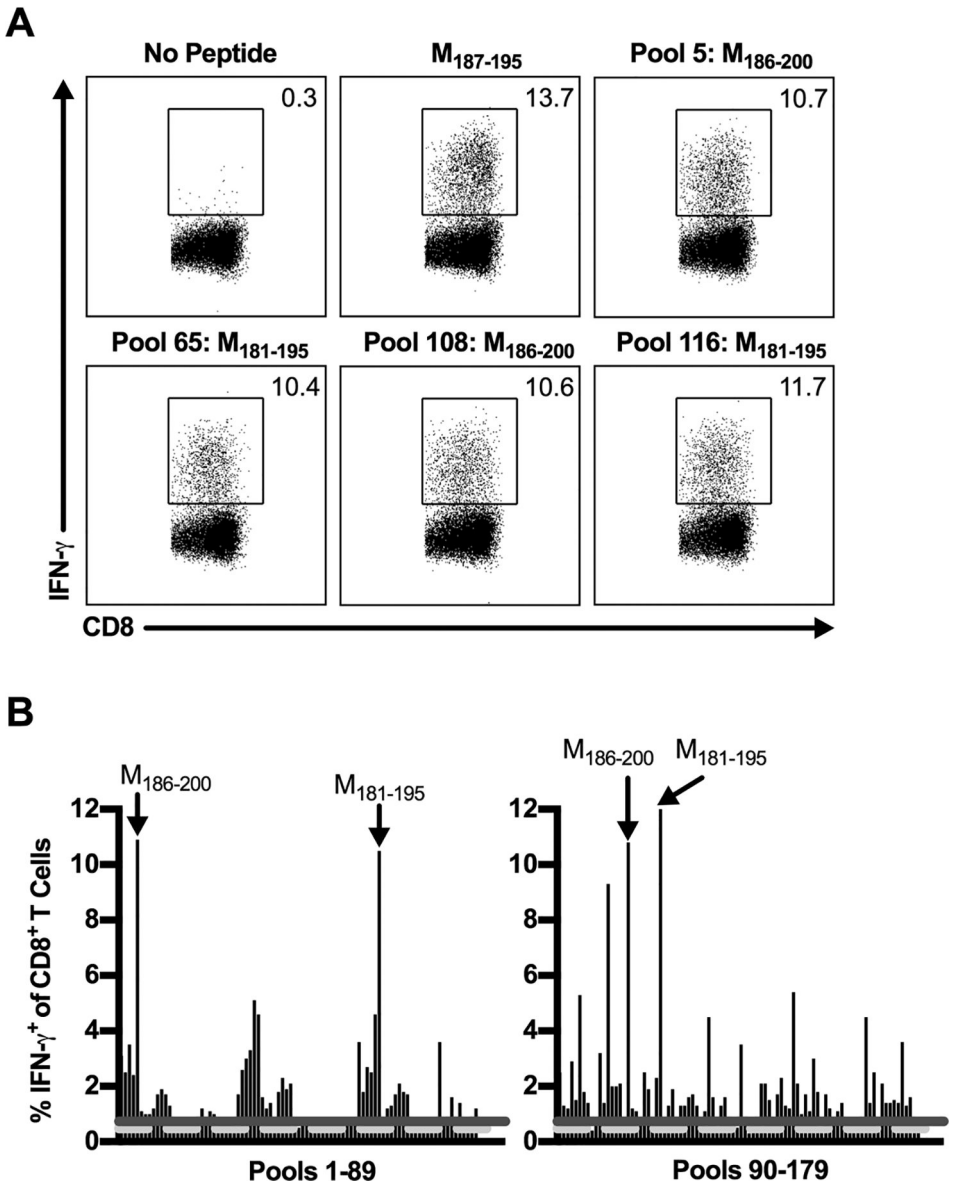

Figure 4. RSV peptide library screen for candidate CD8$^+$ T cell epitopes.

C57BL/6 mice were infected with RSV, and lungs were harvested on day 8 p.i. Lung cells were either incubated with BFA alone or stimulated with a pool containing 10 individual RSV-derived peptides from a peptide library spanning the entire RSV proteome. **(A)** Dot plots show the frequency of IFN-γ^+ CD8$^+$ T cells elicited following peptide stimulation with the previously defined CD8$^+$ T cell epitope, $M_{187–195}$, or pools containing its corresponding peptides in the peptide library, $M_{181–195}$ and $M_{186–200}$. **(B)** The frequency of IFN-γ^+ CD8$^+$ T cells induced by peptide stimulation with all peptide pools. The dashed light gray line represents the average of no peptide controls (y=0.47), and the solid dark gray line represents the 3-SD threshold for positivity (y=0.73). Arrows indicate pools containing the previously defined $M_{187–195}$ CD8$^+$ T cell epitope. Data are representative of 1 of 2 experiments with 24 mice pooled per experiment.

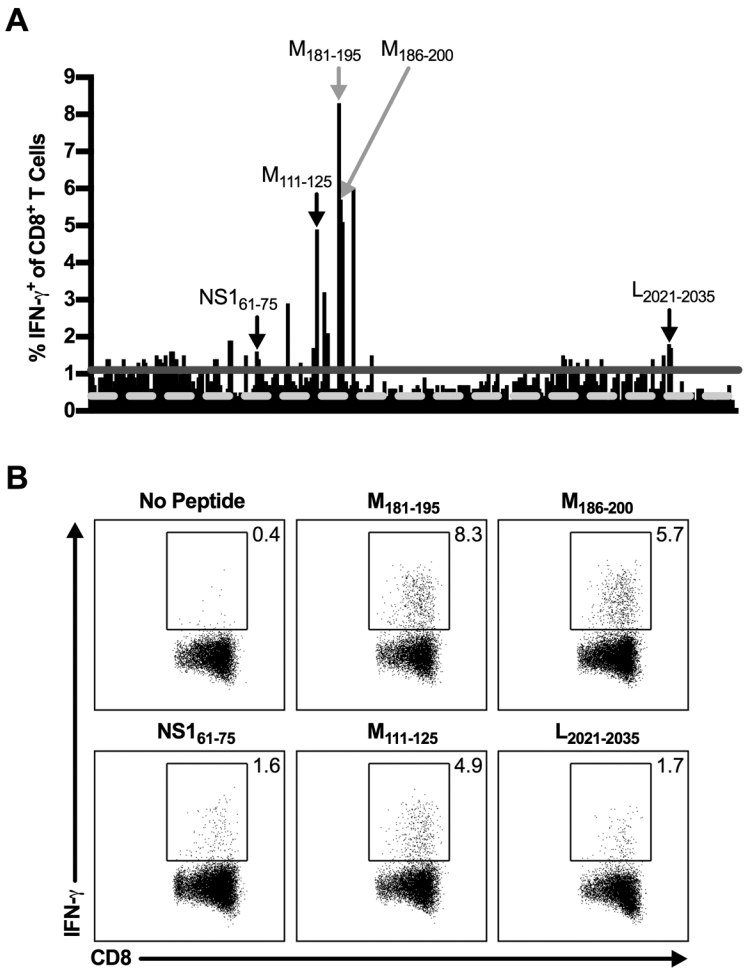

Figure 5. Identification of novel RSV CD8$^+$ T cell epitopes.

C57BL/6 mice were infected with RSV, and lungs were harvested on day 8 p.i. Lung cells were either incubated with BFA alone or stimulated with individual candidate CD8$^+$ T cell epitopes. **(A)** The frequency of IFN-γ^+ CD8$^+$ T cells induced by peptide stimulation with individual candidate CD8$^+$ T cell epitopes. The dashed light gray line represents the average of no peptide controls (y=0.40), and the solid dark gray line represents the 3-SD threshold for positivity (y=1.10). Gray arrows indicate library peptides containing the previously defined $M_{187–195}$ CD8$^+$ T cell epitope. Black arrows indicate select CD8$^+$ T cell epitopes utilized for further study. **(B)** Dot plots show the frequency of IFN-γ^+ CD8$^+$ T cells elicited by select individual peptides that are ≥ the 3-SD threshold for positivity. Data are representative of 1 of 2 experiments with 30 mice pooled per experiment.

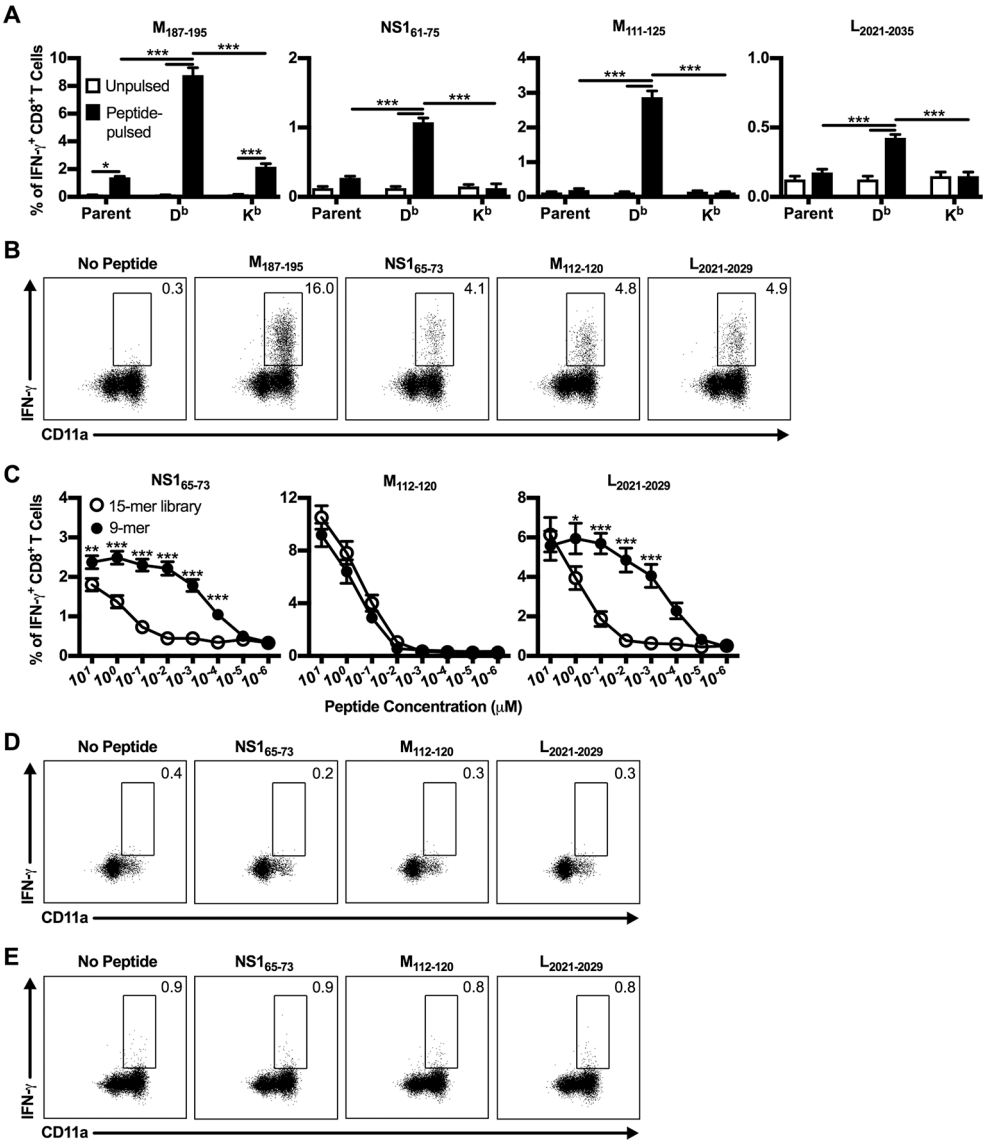

Figure 6. Confirmation of novel RSV CD8$^+$ T cell epitopes.

(A-C) C57BL/6 mice were infected with RSV, and lungs were harvested on day 8 p.i. **(A)** Sort-purified CD8$^+$ T cells were stimulated with either unpulsed (open bars) or peptide-pulsed (closed bars) MHC class I-expressing P815 cell lines at a 2:1 effector-to-stimulator ratio and stained intracellularly for IFN-γ. Parent indicates untransfected P815 cells, and D^b and K^b indicate P815 cells transfected with H-2D^b and H-2K^b MHC class I molecules, respectively. Data are presented as mean ± SEM of 1 of 2 independent experiments (n=4). Groups were compared using two-way ANOVA with Tukey's post-test. **(B)** Lung cells were either incubated with BFA alone or stimulated with CD8$^+$ T cell minimal core epitope 9-mer peptides at a 1 μM concentration and stained intracellularly for IFN-γ. Dot plots are previously gated on CD8$^+$ T cells and show the frequency of IFN-γ$^+$ CD8$^+$ T cells that are CD11a^{hi}. Data are representative of 1 of 4 experiments (n=4–6). **(C)** Lung cells were stimulated with either 15-mer library peptides (open circles) or CD8$^+$ T cell minimal core epitope 9-mer peptides (closed circles) at the indicated peptide concentrations and stained

intracellularly for IFN-γ. Data are presented as mean ± SEM of 2 independent experiments (n=8). Groups were compared using Student's t test. **(D/E)** Lung cells from (**D)** naive C57BL/6 mice or **(E)** day 8 IAV-infected C57BL/6 mice were either incubated with BFA alone or stimulated with $CD8^+$ T cell minimal core epitope 9-mer peptides at a 1 μM concentration and stained intracellularly for IFN-γ. Data are representative of 1 of 2 experiments (n=4). * p<0.05, ** p<0.01, *** p<0.001.

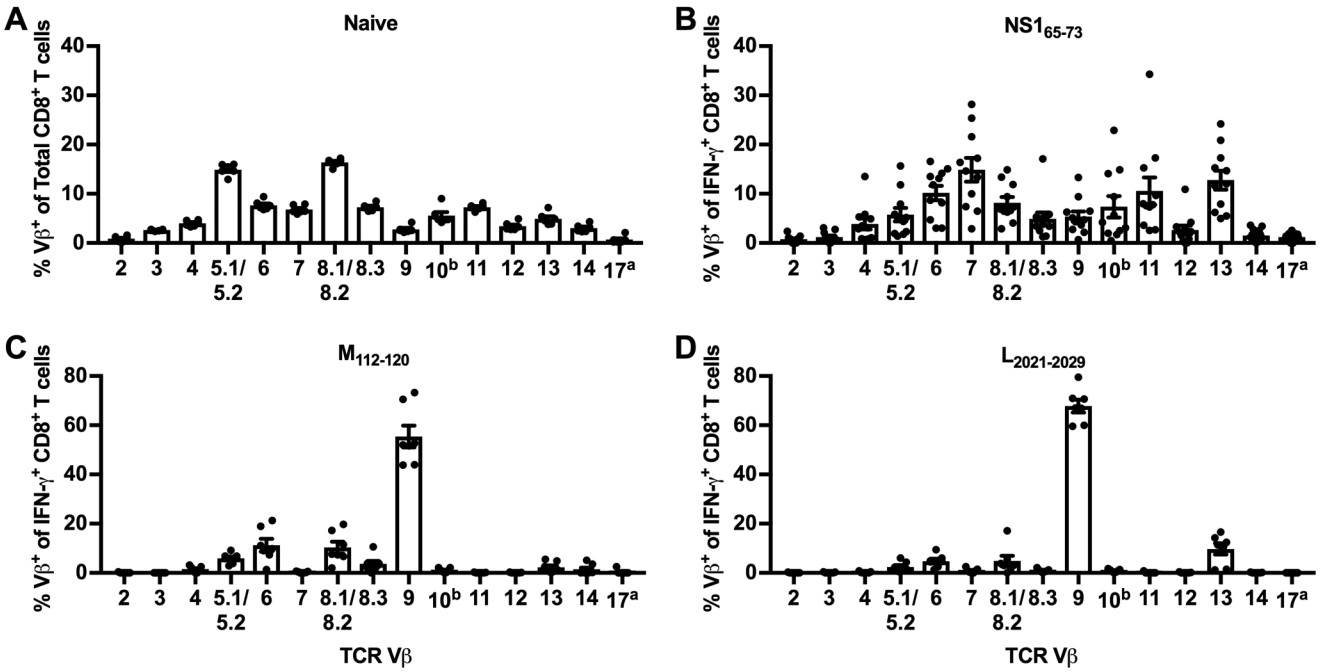

Figure 7. TCR Vβ usage of novel CD8$^+$ T cell epitopes.

(A) TCR Vβ usage of CD8$^+$ T cells in the lungs of naive C57BL/6 mice. **(B/C)** C57BL/6 mice were infected with RSV, and lungs were harvested on day 8 p.i. Lung cells were stimulated with $NS1_{65–73}$, $M_{112–120}$, or $L_{2021–2029}$ peptides, stained extracellularly with a panel of TCR Vβ-specific antibodies, and stained intracellularly for IFN-γ. Lung cells were gated on IFN-γ$^+$ CD8$^+$ T cells and graphs show the TCR Vβ usage of **(B)** $NS1_{65–73}$-, **(C)** $M_{112–120}$-, and **(D)** $L_{2021–2029}$-specific IFN-γ$^+$ CD8$^+$ T cells. Data are presented as mean ± SEM of 2–3 independent experiments. Each dot represents an individual mouse (n=6–11).